Journal Pre-proofs

Liposomes as tunable platform to decipher the antitumor immune response triggered by TLR and NLR agonists

Célia Jacoberger-Foissac, Hanadi Saliba, May Wantz, Cendrine Seguin, Vincent Flacher, Benoît Frisch, Béatrice Heurtault, Sylvie Fournel

Please cite this article as: C. Jacoberger-Foissac, H. Saliba, M. Wantz, C. Seguin, V. Flacher, B. Frisch, B. Heurtault, S. Fournel, Liposomes as tunable platform to decipher the antitumor immune response triggered by TLR and NLR agonists, *European Journal of Pharmaceutics and Biopharmaceutics* (2020), doi: https://doi.org/10.1016/j.ejpb.2020.05.026

This is a PDF file of an article that has undergone enhancements after acceptance, such as the addition of a cover page and metadata, and formatting for readability, but it is not yet the definitive version of record. This version will undergo additional copyediting, typesetting and review before it is published in its final form, but we are providing this version to give early visibility of the article. Please note that, during the production process, errors may be discovered which could affect the content, and all legal disclaimers that apply to the journal pertain.

Liposomes as tunable platform to decipher the antitumor immune response triggered by

TLR and NLR agonists

Célia Jacoberger-Foissac[a], Hanadi Saliba[a], May Wantz[a], Cendrine Seguin[a], Vincent Flacher[b], Benoît Frisch[a], Béatrice Heurtault[a1*], Sylvie Fournel[a1*]

[a] Université de Strasbourg, CNRS, 3Bio team, Laboratoire de Conception et Application de Molécules Bioactives, UMR 7199, Faculté de Pharmacie, 74 route du Rhin, 67401 Illkirch Cedex, France
Email address: bheurtault@unistra.fr (B. Heurtault) and s.fournel@unistra.fr (S. Fournel)

[b] Laboratory I²CT - Immunology, Immunopathology and Therapeutic Chemistry, CNRS UPR 3572, Institut de Biologie Moléculaire et Cellulaire, 15 Rue René Descartes 67084 Strasbourg Cedex, France

[1] Equal contribution

Keywords: therapeutic vaccines, HPV-transformed pulmonary tumors, toll-like and nod-like receptor agonists, liposomal nanoparticles, delivery system

ABSTRACT

Liposomes are powerful tools for the optimization of peptides and adjuvant composition in cancer vaccines. Here, we take advantage of a liposomal platform versatility to develop three vaccine candidates associating a peptide from HA influenza virus protein as CD4 epitope, a peptide from HPV16 E7 oncoprotein as CD8 epitope and TLR4, TLR2/6 or NOD1 agonists as adjuvant. Liposomal vaccine containing MPLA (TLR4 liposomes), are the most effective treatment against the HPV-transformed orthotopic lung tumor mouse model, TC-1. This vaccine induces a potent Th1-oriented antitumor immunity, which lead to a significant reduction in tumor growth and a prolonged survival of mice, even when injected after tumor **appearance.** This efficacy is dependent on CD8^{+} T cells. Subcutaneous injection of this treatment induces the migration of skin DCs to draining lymph nodes. Interestingly, TLR2/6 liposomes trigger a weaker Th1-immune response which is not sufficient for the induction of a

1

prolonged antitumor activity. Although NOD1 liposome treatment results in the control of early tumor growth, it does not extend mice survival. Surprisingly, the antitumor activity of NOD1 vaccine is not associated with a specific adaptive immune response. This study shows that our modulable platform can be used for the strategical development of vaccines.

1. Introduction

Since the beginning of the 20th century, immunotherapy has emerged as an effective strategy to overcome drawbacks of standard cancer treatments by harnessing the innate and specific ability of the immune system to eliminate tumors.[1,2] Among the different types of immunotherapies, therapeutic cancer vaccines showed tremendous beneficial activity in different animal models and are currently evaluated in several large-scale clinical trials.[3–5] Cancer vaccines aim at delivering tumor antigens to dendritic cells (DCs), which will present them in the form of MHC-peptides complex to CD4+ and CD8+ T-lymphocytes. The interaction between those three types of cells results in the differentiation of cytotoxic CD8+ T-lymphocytes (CTLs), able to specifically destroy cancer cells.

Peptide-based vaccine strategies had mainly focused on MHC class-I restricted tumor-specific epitope peptides. Nevertheless, it is admitted that cancer vaccines should as well induce the differentiation of CD4+ T-lymphocytes into T-helper cells (Th) to support the desired immunologic response. To this end, one possibility is the use of heterologous MHC class-II restricted peptide, which stimulates recall non-tumor specific memory CD4+ T cells, thereby creating a favorable environment for tumor-specific CTL differentiation.[6,7] Short peptides used in this strategy have the advantage of low-cost manufacturing and are safe. However, they are non-immunogenic and need to be combined with a potent adjuvant to trigger DC maturation

2

and improve antigen presentation. In the last decade, different Toll-like and Nod-like Receptor (TLR and NLR, respectively) agonists were investigated as vaccine adjuvants and showed promising results in clinical studies.[8] In particular, the monophosphoryl lipid A (MPLA, a TLR4 agonist) has already received FDA approval and is commercialized by GlaxoSmithKline as adjuvant system in combination with liposomes (AS01).[9]

In this context, we developed a vaccination platform made of lipid nanoparticles (liposomes), **where the same nanoparticle contains** both MHC class-I and class-II epitope peptides **as well as an** agonist of TLR or NLR. In our platform, the CD8$^+$ T cell peptide epitope (referred as CD8 epitope) is a tumor-specific peptide, enabling a cytotoxic response restricted to tumor cells. The CD4$^+$ T cell peptide epitope (referred as CD4 epitope) **is a universal helper peptide, which binds a wide range of MHC class-II human and mouse alleles and is derived from a pathogen sufficiently widespread to ensure the presence of memory cells in a large part of the human population for a future clinical application of our platform.[10,11]** Once optimized, the CD8 epitope present in our construct might be tunable in order to address different types of cancer.

In a previous study, we evaluated liposomes co-delivering ErbB2-derived CD8$^+$ peptide epitope, a universal helper peptide from influenza virus, and a synthetic TLR2/6 agonist (Pam$_2$CAG) in a mouse model of subcutaneously implanted renal carcinoma (RenCa) expressing human ErbB2 protein. Subcutaneous administration of this construct led to a potent antitumor activity in both prophylactic and therapeutic injection schedules.[12,13]

These encouraging results prompted us to exploit the versatility of our construct to decipher the antitumor immune response induced by our vaccination platform in a model of HPV (human papillomavirus)-16 transformed cancer cells. For this, three peptide-based liposomal vaccines

were conceived, containing two epitopes: a tumor-specific CD8$^+$ peptide derived from the HPV16 E7 oncogene and an influenza-derived CD4$^+$ peptide used in our previous studies in association with TLR2/6, TLR4 or NOD1 agonists. **Each nanoparticle in theses vaccines contained the three elements required to induce a potent immune response (adjuvant, CD4 and CD8 epitopes)**. The antitumor activity of these three vaccine candidates was assessed against the TC-1 cell line, which is E7-transformed tumor cells derived from murine pulmonary epithelial cells. In addition to having an identified tumor-associated antigen (TAA), TC-1 cell line is also a well-described preclinical model for human tumors transformed by HPV, such as non-small-cell lung cancer (NSCLC) or cervix cancer, which are amongst the deadliest cancer forms in the world.[14,15] The therapeutic effect and the immune responses induced by our three constructs were deciphered in vivo after s.c. injections at different stages of cancer progression.

2. Materials and methods

2.1. Lipids, adjuvants and peptides

Egg yolk L-α-phosphatidylcholine (PC), and cholesterol (Chol, recristallized in methanol) were purchased from Sigma-Aldrich (St. Louis, MO). Egg yolk *L*-α-phosphatidyl-*DL*-glycerol (PG) was purchased from Avanti Polar lipids. Lipids purities exceeded 99%. The lipopeptide S-[2,3-bis(palmitoyloxy)-(2R)-propyl]-(R)-cysteinyl-alanyl-glycine (Pam$_2$CAG) and the thiol-reactive dipalmitoylglycerol-maleimide anchor (DPGmal) were synthesized in the laboratory as previously described.[16,17] The lipopolysaccharide derivative monophosphoryl lipid A (MPLA) and the acylated derivative of the dipeptide γ-*D*-Glu-mDAP (C12iEDAP) were purchased from Invivogen (San Diego, CA). All reagents were conserved under argon atmosphere at -20 °C, in a powder form or dissolved in chloroform/methanol (9/1, v/v). Synthetic peptides were obtained from Genosphere Biotechnologies (Paris, France). The

influenza virus haemagglutinin-derived peptide, HA 307–319 (PKYVKQNTLKLAT-C), refers to CD4 epitope. The peptide derived from HPV16 oncogene protein, E7 49-57 (RAHYNIVTF-C), refers to CD8 epitope. MART 27-35 (AAGIGILTV) is an irrelevant peptide for this tumor model and was used as negative control during ELISpot assay.

Formulation of liposomes: Multilamellar vesicles (MLV) were prepared by lipid film hydration technique as described previously.[18] Briefly, a chloroform/methanol solution (9/1, v/v) containing a mixture of lipids, adjuvant and/or DPGmal anchor were mixed in a round-bottom Pyrex tube, and were completely dried under high vacuum for 45 min. Molar ratios of each component are shown in Table 1. The resulting lipid film was then hydrated in 10 mM Hepes buffer (pH 6.5) containing 5% (w/v) sorbitol at a final phospholipid concentration of 15 mM, leading to the formation of MLV. This suspension was then sonicated (1 s cycle every 3 s) during 1 h at room temperature under a continuous flow of argon, using a Vibra Cell 75041 ultrasonicator (750 W, 20 kHz, Fisher Bioblock Scientific, Waltham, MA) equipped with a 3 mm-diameter tip probe (40% amplitude). The resulting small unilamellar vesicle (SUV) preparations were centrifuged at 13,000 g for 15 min to remove the titanium dust originating from sonication probes.

2.2. Peptide conjugation to liposomes

Peptides were first dissolved in milliQ water and potential disulphide bonds were reduced in presence of 0.7 M eq. tris(2-carboxyethyl) phosphine hydrochloride (Sigma-Aldrich) for 15 min under argon at RT. Equimolar quantities of CD4 and CD8 peptide epitopes were then coupled to preformed DPGmal-containing SUV by Michael addition at pH 6.5 (0.5 molar eq. of each peptide compared to surface accessible thiol-reactive maleimide functions). After 4 h under argon at room temperature, a 10-fold excess of β-mercaptoethanol was added for 30 min

to inactivate all unreacted maleimide groups on internal and external surface of SUV. Then, the formulation was extensively dialyzed (Spectra/Por, exclusion limit of 12–14 kDa, Spectrum laboratories, Breda, Netherlands) against a 10 mM Hepes buffer (pH 7.4) containing 5% (w/v) sorbitol to eliminate unconjugated peptides and excess of reagents. Finally, 4% glucose (w/v) was added as a cryoprotectant and formulations were snap frozen in liquid nitrogen and stored at -80 °C until further usage.

2.3. Physicochemical characterization of liposomal constructs

The average diameter of formulated liposomes was measured by dynamic light scattering using a Zetasizer Nano-ZS (Malvern instruments, Orsay, France) with the following specifications: viscosity: 1.014 cP; refractive index: 1.34; scattering angle: 90°; temperature: 25 °C. SUV were diluted at 1/100 in 10 mM Hepes buffer (pH 7.4) containing 5% (w/v) sorbitol, and the results presented are the average of 8 independent formulations (with three consecutive measurements per formulation). Data were analyzed using the multimodal number distribution software included with the instrument. Particle size is expressed in intensity. Sample are considered monodispersed when the polydispersity index (PDI) is < 0.3.

Zeta potential of liposomes was determined at 25 °C using a Zetasizer Nano-ZS. The samples were dispersed at 1/100 in 10 mM Hepes buffer containing 5% (w/v) sorbitol (pH 7.4) and the zeta potential was calculated from the electrophoretic mobility based on the Smoluchowski approximation.

The PC content of formulated liposomes was determined using an enzymatic assay with the LabAssay™ Phospholipid kit (Wako Pure Chemical industries Ltd). Briefly, 1-2 μL of SUV were incubated with 200 μL of the enzymatic reagent in triplicates in a 96-well plate. The reagent contains a phospholipase C that releases the choline, which is then oxidized by the

choline oxidase. The reaction produces hydrogen peroxide needed by the peroxidase to convert a chromogen into a blue product. After 10 min at 37 °C, absorbance was measured at $\lambda = 595$ nm using a microplate reader (Safas SP2000, Xenius 5801, Monaco). PC content in each sample was determined from a calibration curve prepared with purified choline chloride.

The quantification of conjugated peptides in each formulation was performed using fluorescamine (4-Phenylspiro-[furan-2(3H),1-phthalan]-3,3′-dione, Sigma-Aldrich) in a fluorometric assay. Briefly, amino acids were generated during acid hydrolysis of peptide-conjugated liposomes by the addition of 12N HCl, at 110 °C for 12 h in a heating module (Pierce Reacti Therm III™, Thermo Fisher scientific). After neutralization by the addition of 6N sodium hydroxide, 20 μL of the hydrolysis solution was added to 750 μL of 50 mM sodium borate buffer (pH 9), followed by the addition of 250 μL of fluorescamine solution in dioxane (300 mg/L). Fluorescence was measured immediately at λexcitation = 400 nm and λemission = 480 nm. A physical mixture of plain liposomes and peptides were used to establish a calibration curve. Coupling rates were calculated relative to the quantity of surface-exposed maleimide functions.

2.4. Animals

Specific-pathogen-free 6-8 week old male C57BL/6J mice were purchased from Charles River Laboratories. In vivo experiments were performed in full compliance with the CEE directive 2010/63/EU adopted on 22 September 2010, relating to the protection of animals used for experimental purposes and was done in compliance with the French law (décret n° 2013–118, 1 February 2013). Experiments were performed with the approval of the local Animal Care and Use Committee of Alsace (authorization number: APAFiS #10825- 2017073117337272).

2.5. Tumor cell line

7

All the reagents use for cell culture were purchased from Sigma-Aldrich. TC-1 cells, expressing E7 protein from HPV16, were obtained from ATCC® (CRL-2785™). TC-1 cell line was derived from pulmonary epithelial cells of C57BL/6J mice, immortalized by transduction of the LXSN16E6E7 retroviral vector and subsequently transformed with the pVEJB plasmid expressing activated human c-Ha-*ras* gene.[19] Cells were cultivated in RPMI 1640 culture medium supplemented with 10% heat-inactivated fetal calf serum (FCS), 100 UI/mL penicillin and 100 μg/mL streptomycin and were incubated at 37 °C in 5% CO_2, 80% humidity.

2.6. In vivo evaluation of liposome-based vaccines

A total of 1×10^5 TC-1 cells were injected intravenously in the tail vein of C57BL/6J mice in 100 μL normal saline solution, except for DC subsets analysis, which was performed on tumor-free mice. In each experiment, mice received two sc. immunizations in the right flank at 2-days interval. Treatments with liposomal vaccines contained 15 μg E7 peptide or an equivalent amount of lipids (~1 mg) for plain liposomes (negative control). The interval between tumor injection and therapeutic vaccinations varied as specified in each figure legends.

CD4 and CD8α depleting antibodies (GK1.5 and 53-6.72 clones respectively) were purchased from eBioscience (Thermo Fisher Scientific, Waltham, MA). Depletions of CD8$^+$ or CD4$^+$ cells were performed by a single i.p. injection of 200 μg depleting antibodies one day before tumor implantation, followed by a weekly recall injection. Purified IgG from rat serum (Sigma-Aldrich) was injected into control mice. Blood was sampled from the submandibular vein of the cheek pouch with a 5-mm lancet to monitor the depletion of CD8$^+$ or CD4$^+$ T cells at day -3, 7, 14 and 21 by flow cytometry analysis of peripheral blood mononuclear cell (PBMC).

Mice bearing tumors were culled at day 28 after tumor injection (except for survival experiments) or whenever they showed signs of pain and discomfort. Spleen, lymph nodes

draining the site of injection and lungs were harvested for the evaluation of antitumor immunity or tumor growth progression. Mice lungs were contrasted by intratracheal injection of 15% India Ink solution, followed by bleaching into a Fekete's solution. For each mouse, the number of white tumor nodules on the black surface of lungs was counted using a magnifier lamp.

For DC subsets migration and activation analysis, negative and positive control groups were added: untreated mice or cholera toxin injection (2 μg/dose, Sigma-Aldrich). Tumor-free C57BL/6J mice received only one treatment injection and 48 h after, inguinal draining lymph node (DLN) from the right flank were harvested for digestion, labeling and flow cytometry analysis.

2.7. Lymph node and spleen cell suspension preparation

DC subsets analysis: DLN cell suspension was obtained by mechanical disruption, digestion (Collagenase D, DNAse I, Roche Applied Science) for 1 h at 37 °C and filtration on 100 μm nylon mesh cell strainer.

ELISpot and ELISA assays: Spleen and lymph nodes draining the injection site (axillary and inguinal) from the same group treatment were pooled, dissociated and filtered onto a 70 μm nylon mesh cell strainer (BD Biosciences, Franklin Lakes, NJ). Resulting cell suspensions were centrifuged at 200g for 5 min and lymph node cell pellet was resuspended in RPMI medium, where FCS is replaced with 2% normal mouse serum (Dominique Dutscher, Brumath, France). To remove red blood cells, the spleen cell pellet was resuspended in ammonium-chloride-potassium (ACK) lysing buffer (0.15 M NH_4Cl, 1 mM $KHCO_3$, and 0.1 mM EDTA, pH 7.4) at room temperature for 30 s. ACK was diluted 10 times in RPMI to stop the lysis, centrifuged and the spleen cell pellet was resuspended in RPMI 2% normal mouse serum. Cells were counted and diluted before used in further *ex vivo* experiments.

2.8. IFN-γ ELISpot assay

PVDF membrane 96-well plates (Multiscreen® HTS filter plates, Merck Millipore) were activated with 35% ethanol and coated with purified anti-mouse IFN-γ (clone AN-18, eBioscience) in PBS overnight at 4 °C. After three washes, membranes were blocked with RPMI 10% FCS for at least 2 h at 37 °C, and washed again with RPMI without FCS. Spleen or DLN suspensions were cultured in triplicates (4.10^6 cells/mL), in presence of recombinant human IL-2 (30 UI/mL), with CD4$^+$ or CD8$^+$ T cell epitopes (10 µg/mL), irrelevant peptide (10 µg/mL) or TC-1 tumor cells (125.10^3 cells/mL). Cells cultured in medium alone or with 1.25 µg/mL of concanavalin-A (Sigma-Aldrich) were used as negative and positive controls, respectively. After 20-24 h at 37 °C, 5% CO_2, plates were washed with PBS 0.01% Tween 20 and immunospots were revealed using consecutive incubations with biotinylated anti-IFN-γ detection antibody (clone R4-6A2, eBioscience), alkaline phosphatase-conjugated extravidin and BCIP/NBT solution (Sigma-Aldrich). Spots were counted using a Bioreader 4000 PRO-S (Biosys, Karben, Germany). The number of spots obtained with the negative control (medium alone) was subtracted from other conditions, normalized per 10^6 cells and averaged for each triplicate.

2.8. ELISA

Cytokine levels in spleen cell supernatants were measured by ELISA, after 72 h incubation in the same conditions as IFN-γ ELISpot assay. IFN-γ, IL-5, IL-13 (eBioscience) and IL-17 (R&D systems, Minneapolis, MN) antibody pairs and standard were used at concentrations recommended by manufacturers. Briefly, purified antibodies in a 0.05 M pH9.6 carbonate/bicarbonate buffer were adsorbed on ELISA plates (Microlon™, Greiner Bio-One) overnight at 4 °C, before blocking with PBS 0.05% Tween 20 containing 1% BSA (1 h, 37°C).

10

50 μL of supernatants in duplicate were then incubated (2 h, 37°C), followed by incubations with biotinylated antibodies detection in blocking buffer (1 h, 37°C). Horseradish peroxidase-conjugated streptavidin was then added (45 min, 37°C) and revelation was conducted by adding a solution of 1.25 mM tetramethylbenzidine and 13.05 mM H_2O_2 in 0.1 M pH 5 citrate buffer. After 15 min, enzymatic reaction was stopped by the addition of 1 M HCl and the absorbance was read at 450 nm with a spectrophotometer (Safas SP2000, Xenius 5801, Monaco). Fold change was determined by dividing the amount of cytokine observed under each condition by the one obtained with negative control (medium alone).

2.9. Flow cytometry analysis

For DC subsets analysis, anti-Langerin/CD207-AF488 (clone 929F3.01) (Dendritics, Dardilly, France), anti-CD103-PE (clone M290), anti-CD8α-PercP/Cy5.5 (clone 53-6.7), anti-CD11c-PE/Cy7 (clone HL3) (BD Pharmingen™), anti-CD86-APC (clone PO3), anti-MHC class II (I-A/I-E)-Alexa700 (clone M5/11415.2) (Biolegend, San Diego, CA) antibodies were used for flow cytometry at concentrations recommended by manufacturers.

Prior to antibody staining, dead cells were labelled with FVD-eFluor450 (eBioscience) and Fc-receptors were blocked with FcR blocking reagent (Miltenyi Biotech, Bergisch Gladbach, Germany) for 15 min. Cells were then incubated with the staining antibodies during 30 min at 4°C. For cell permeabilization and fixation, the pellets were resuspended in BD Cytofix/Cytoperm™ buffer followed by an internal staining with anti-Langerin-AlexaFluor488 for 30 min at 4 °C. Data were acquired on a Gallios flow cytometer (Beckman-Coulter, Brea, CA) and analysis was performed with Flowjo® software (version 10.2, Ashland, OR).

The efficiency of CD8+ or CD4+ cells depletion was monitored by flow cytometry analysis of peripheral blood mononuclear cells. Blood samples from the submandibular vein of the cheek

pouch of mice were collected into *Capiject* tube (Terumo T-MQK). To remove red blood cells, uncoagulated blood was resuspended in ammonium-chloride-potassium (ACK) lysing buffer (0.15 M NH_4Cl, 1 mM $KHCO_3$, and 0.1 mM EDTA, pH 7.4) and incubated at room temperature for 10 min. After centrifugation and washing into cold PBS 2% FCS, the white blood cell pellet was incubated with @CD16/CD32 (clone 93, eBioscience) for 10 min at 4°C. Then the cells were stained with the following antibodies, used at concentrations recommended by the manufacturer: anti-CD4-FITC (clone RM4-4) and anti-CD8b.2-APC (clone 53-5.8) (Biolegend). BD FACSCalibur™ (BD Biosciences) was used for flow cytometry acquisition and analyses were performed with the FlowJo® software (version 10.2, Ashland, OR).

2.10. Statistical analysis

All data are presented as mean±SEM and were calculated with the GraphPad Prism 7.0 software. Statistical differences obtained in the ELISpot assay, depletion experiments and DC subsets analysis were determined by a two-way ANOVA with Dunnett's multiple comparison *posthoc* test. A One-way Anova was performed for the comparison of tumor count and ELISA protein fold change; a nonparametric test (Kruskal-Wallis) was used instead when recommended. Survival curves were compared with a Log-rank test. Difference between groups was considered statistically significant for p<0.05 (one symbol), p<0.01 (two symbols), p<0.001 (three symbols) or p<0.0001 (four symbols).

3. Results

3.1. Physicochemical characterization of liposomal constructs

Three liposomal formulations were conceived, containing **within the same nanoparticle** two peptide epitopes, HA peptide (MHC class-II restricted) derived from hemagglutinin A influenza

12

virus protein, and E7 peptide (MHC class-I restricted) derived from HPV16 oncoprotein, in association with one type of adjuvant: TLR2/6, TLR4 or NOD1 agonists **(Table 1)**. These constructs were characterized to determine their physicochemical properties. Additionally, the amount of peptides and agonist was determined **(Table 2)**. Each liposomal formulation exhibited a uniform size distribution with a mean diameter around 70 nm for plain liposomes (negative control, without peptides and agonist) and 83 nm for liposomes with peptides and adjuvant, regardless of their composition. The surface charge was invariably negative (-51 to -61 mV) and the peptide binding rate to the surface of liposome always exceeded 78%. According to the literature, these specific features (size below 100 nm and negative surface charge) will allow them to be efficiently drained by the lymphatic system or endocytosed rapidly by DCs at the site of injection.[20,21]

3.2. TLR4 liposomes treatment induces a long-lasting antitumor activity and a better mice survival

To evaluate the antitumor activity of vaccine candidates in the TC-1 orthotopic pulmonary tumor model, therapeutic vaccinations were performed after injection of TC-1 cells in the tail vein of C57BL/6J mice. Given that pulmonary nodules were detectable 8 days after TC-1 cells i.v. injection **(Fig. S1)**, vaccine candidates were injected at various time points, ranging from day 2 to day 14, in order to evaluate their therapeutic effect at different stages of cancer progression. One month after tumor cell injection, lungs were harvested and contrasted for pulmonary tumor nodules counting. Liposomal vaccine containing the TLR2/6 agonist was no longer effective when injected 8 days after tumor injection **(Fig. 1A)**. In contrary, liposomes containing TLR4 or NOD1 agonists were able to reduce the tumor growth even when injected after pulmonary nodules **appearance,** up to an efficiency limit at day 12 **(Fig. 1B and 1C)**.

Survival rate of mice treated with the three vaccine candidates was assessed after therapeutic injections during an early stage of cancer progression (days 2-4) or after the **appearance** of pulmonary nodules (days 10-12). Consistent with the previous observations, treatment with TLR2/6 liposomes increased survival only of animals treated at days 2-4 **(Fig. 1D)** but was ineffective when the treatment was administered after nodules **appearance (Fig. 1E)**. TLR4 liposomes were significantly efficient in both administration schedules. Strikingly, when injected at days 10-12, this vaccine allowed complete tumor regression in more than 50% of the mice, which remained pulmonary nodules-free after 3 months (**Fig. 1E**). Surprisingly, NOD1 liposomes failed to extend survival under both schedules (**Fig. 1D and 1E**), although a decrease of nodule numbers was observed 28 days after tumor cells injection (**Fig. 1A**). This suggests that the three vaccines induced antitumor responses that differ in a quantitative and/or qualitative way.

3.3. TLR4 liposomes induces a strong Th1 antitumor immune response

To better understand the difference of therapeutic efficacy previously observed, we compared the tumor-specific adaptive immune response induced by the three vaccine candidates in tumor-bearing mice. Therapeutic vaccinations were performed at days 2-4 after i.v. injection of TC-1 cells. One month later, the systemic (spleen) and local immune responses (lymph nodes draining the injection site) were evaluated by *ex vivo* counts of IFN-γ producing T cells reacting to vaccine epitopes or tumor cells in an ELISpot assay. A high number of E7-specific IFN-γ producing T cells were observed in mice treated with TLR2/6 liposomes in the spleen but not in the lymph nodes **(Fig. 2A)**. On the other hand, TLR4 liposomes induced a significant adaptive immune response in both the spleen and lymph nodes. In consistence with mouse survival results (**Fig. 1D and 1E**), NOD1 liposomes failed to induce the differentiation of a

14

high number of E7 specific IFN-γ producing T cells, in both lymphoid organs. A TC-1-specific response was only observed after TLR4 liposome treatment.

In the Fig. 2A, no IFN-gamma response to the HA peptide could be detected. However, this was already shown previously that HA-containing liposomes were able to induce a very strong CD4$^+$ T cell response in this mouse model.[18] The main reason to explain the lack of immune response against the CD4 epitope is the fact the injection schedule used in this work is not appropriate for the analysis of a CD4$^+$ T-cell response, classically measurable between 7 and 11 days after immunization.[22-24] In this publication, the immune response was analyzed more than 2 weeks following vaccine injection, to detect CD8$^+$ T-cell response against the E7 peptide and the tumor cells.

Th1 polarization is mandatory for the differentiation of potent CTLs or the activation of innate cytotoxic immune cells and has been correlated with a better cancer vaccine efficacy.[25] Therefore, immune response polarization was evaluated by ELISA on the supernatant of splenocyte cultures, by measuring hallmark cytokines for different Th cells subsets: IFN-γ (Th1 response), IL-5 and IL-13 (Th2 response) and IL-17 (Th17 response). In a similar way to the ELISpot assay, we observed a strong IFN-γ production in spleen supernatants from mice treated with TLR4 liposomes, incubated in presence of E7 peptide **(Fig. 2B)** or TC-1 tumor cells **(Fig. 2C)**. This potent Th1 immune response was associated with a lack of IL-5, IL-13 and IL-17 cytokines within this treatment group. The same tendency was observed for TLR2/6 and NOD1 liposomes, which also promoted IFN-γ production, although at a lower amount. Thus, the vaccine efficacy in our model is correlated with a significant production of IFN-γ, reflecting Th1 polarization of the immune system. These results confirmed the superiority of TLR4

15

liposomes, which are able to trigger a potent antitumor immunity (**Fig. 2**) in association with a significant tumor regression and improved mice survival (**Fig. 1**).

3.4. CD8$^+$ and CD4$^+$ T cells depletion differentially impact the therapeutic effect of adjuvanted liposomes

In the context of vaccine-induced antitumor immunity, IFN-γ can be produced by CTLs or Th1 cells. Therefore, we investigated the importance of CD8$^+$ and CD4$^+$ T cells for the therapeutic activity of our peptide-based liposomal vaccines. Antibody-mediated depletions of each cell types were performed prior to vaccine and tumor injections, and maintained by a weekly challenge until the end point **(Fig. S2A)**. Depletion of CD8$^+$ or CD4$^+$ T cells was confirmed by flow cytometry analysis of PBMC **(Fig. S2B)**. Depleted and control mice treated with rat IgG received TC-1 cells i.v. injection, followed by two therapeutic administrations of liposomal candidates at days 2 and 4. As expected, treatments with the three peptide-based vaccines induced a significant tumor regression in IgG-treated mice, which was abolished in CD8$^+$ T cell-depleted mice **(Fig. 3A)**. This decrease of therapeutic efficacy was consistent with a clear reduction of tumor-specific IFN-γ-producing T cells in the spleen and lymph nodes, in response to E7 peptide **(Fig. 3C and 3D)** and TC-1 tumor cells **(Fig. 3E and 3F)**. In contrast, CD4$^+$ T cell depletion improved vaccine efficacy, as shown by the decreased number of lung tumor nodules in comparison with their rat IgG-treated counterparts **(Fig. 3B)**. This effect is most likely linked to the simultaneous depletion of CD4$^+$ T helper and Treg cells, which relieved the tumor microenvironment from one of his major suppressive mechanism. Thanks to the depletion experiments, we demonstrated the importance of CD8$^+$ T cells for our vaccines efficacy, which acted at least partially by inducing the proliferation of tumor-specific CTLs.

3.5. Adjuvanted liposomes promote the activation and migration of skin dendritic cells into the draining lymph nodes.

In order to induce a potent T cell differentiation, antigen-loaded skin DCs should become mature and migrate into draining lymph nodes (DLNs) after having encounter adjuvanted-vaccines injected subcutaneously. Ideally, these antigen-presenting cells should be able to perform cross-presentation of E7 peptide by MHC-I molecules. Dermal cDC1 (CD103+ Langerin+) and CD8α+ lymph node (LN)-resident DCs were described as the most efficient cross-presenting DCs.[26,27] Although other skin DC subsets, including epidermal **Langerhans** cells (LCs) and cDC2, might show potency under certain maturation conditions.[27–29]

For these reasons, we characterized skin-derived and LN-resident DC subsets in DLN following liposomal vaccination. We quantified the migration of DCs from the skin by assessing their frequency inside DLNs and the activation status of all subsets by measuring their expression of the maturation marker CD86. DLNs were harvested 48 h after a single s.c. injection of the different constructs and the percentage of four DC subsets was subsequently examined by flow cytometry (**Fig. 4,** using the gating strategy in **Fig. S3**). Cholera toxin was used as positive control in our experiment, since it induces potent dermal DC activation and migration.[30] Two days after vaccine injection, we observed the migration and maturation of skin DCs into the DLNs by comparing them to the negative control group (plain liposomes). We did not observe any variation of lymph-node residing DCs, in particular CD8α+ DCs, in term of frequency or CD86 surface expression. TLR4 liposomes were the only vaccine able to induce a strong migration of Langerin− CD103− cDC2 into the DLN, which was similar to positive control group treated with cholera toxin **(Fig. 4A)**. Surprisingly, CD86 expression of migratory cDC2 after TLR4 liposome injection was not significantly affected **(Fig. 4B-C and Fig. S4)**. These results indicate that the adjuvants in our constructs should preferentially act by increasing the

17

number of migratory, potentially antigen-loaded DCs from the skin, rather than boosting the maturation status of migratory or resident DCs. Interestingly, the least potent vaccine candidate, TLR2/6 liposomes, did not modify the frequency of migratory DCs (**Fig. 4A**), yet triggered a strong activation of dermal cDC1 and cDC2 (**Fig. 4B-C and Fig. S4**). NOD1 liposomes had no significant impact on the migration or activation of DCs, and Langerhans cells appeared unaffected by our different vaccines.

4. Discussion

Taking advantage of a liposomal platform created by our laboratory, we recently defined the optimized epitope composition and adjuvant doses of three peptide-based antitumor vaccines, which differed only by their adjuvant composition.[18] The hereby report sought to evaluate the therapeutic activity of these constructs in a preclinical model of HPV-transformed tumors, and to gain more insight into their immunological mode of action by evaluating in vivo the immune response polarization and immune cells involved in their activity. For this, we studied the development of CD4$^+$ and CD8$^+$ T cell responses. Moreover, because DCs express different Toll-like or Nod-like receptors depending on their origin or phenotype, we determined which DC subsets are affected by the various adjuvants of the three peptide-based vaccines.[31,32]

Among the three vaccine candidates evaluated, MPLA containing-liposomes (TLR4 agonist) were undoubtly the most effective treatment against TC-1 orthotopic pulmonary model. This vaccine significantly reduced the tumor growth when administered up to 2 weeks after tumor cells injection. This is an impressive result given the fact that pulmonary nodules were detectable 8 days after i.v. injection of TC-1 cells and that the rapid growth of this cell line led to the death of untreated mice around day 30. TLR4 liposomes induced a long-lasting antitumor activity associated with a better survival of mice, which was strikingly more effective when

injected at a later stage of cancer (Figure 1E). We assumed that the growing tumor nodules may promote antitumor immune responses by providing an antigen source and inducing inflammation. Indeed, it was already shown in preclinical and clinical studies that immune checkpoint inhibitors[3,33] or vaccines[34,35] had a greater therapeutic efficacy before tumor surgery. **Interestingly, the TLR4 liposomes were more effective, even though the liposomes contained very low dose of adjuvant (0.2μg/injection). An elegant study from Blander & Medzhitov showed that the presence of TLR4 ligand on peptide bearing microspheres highly improved the phagocytose, generation of peptide-MHC class II complexes and the antigen presentation by DC.[36] This new mechanism link to TLR4 signaling may also explain the superiority of the TLR4 liposomes as cancer vaccine**

TLR4 liposomes triggered the induction of a systemic and local Th1 response, associated with a unique production of IFN-γ by immune cells, observed in cell supernatants as well as in ELISpot assay. As expected, depletion of CD8^{+} T cells drastically decreased the antitumor immune response, whereas depletion of CD4^{+} T cells did not. This last observation was very surprising given the expected requirement of CD4^{+} Th1 cells for the maturation of CD8^{+} cytotoxic T cells. Nevertheless, CD4^{+} T cell depletion also affects the CD4^{+} Foxp3^{+} Treg responsible for the dampening of CD8^{+} T cells maturation and proliferation.[37,38] The decrease in Treg cells triggered in our depletion experiment might have induced the conversion of "cold" to "hot" tumors, hence limiting the requirement of helper T cells for CTLs to reduce the tumor growth.[39]

HPV-transformed tumors such as cervical cancer and non-small-cell lung cancer (NSCLC) are amongst the deadliest cancer type. HPV oncogene protein E7 is responsible for the cellular transformation and its expression by tumor cells provides a recurrent antigen to be targeted by

19

cancer vaccines. This study was performed on a E7-transformed cell line derived from mice pulmonary epithelial cells, the TC-1 cell line, which had proven to be an accurate preclinical model for the prediction of human vaccines efficacy.[40,41] Various E7 antigen-based vaccines were already assessed against subcutaneous or orthotopic pulmonary TC-1 tumors such as recombinant virus,[42–46] Shiga toxin B-subunit protein fusion,[47] dendritic cells,[48,49] mRNA or DNA vaccine,[50–52] syngeneic cells,[53] whole protein with complete Freund's adjuvant,[54,55] and synthetic long peptides.[56] Most of these studies reported a great efficacy, both in prophylactic and challenge experiments. However, in primary tumor-bearing mice, we are not aware of any E7-based vaccine preparation demonstrating a therapeutic effect and long-lasting antitumor activity comparable to the TLR4 liposomes.

The Pam_2CAG, used as TLR2/6 agonist, was the least effective adjuvant against TC-1 orthotopic lung tumors. However, in our previous studies using an ectopic model of s.c. implanted RenCa cells, TLR2/6 liposomes have shown a clear efficacy during early stages of tumor progression.[12,13] In the literature, TLR2-targeting formulations were rarely used in therapeutic vaccination, given the variable $CD4^+$ T cell polarization triggered by TLR2 activation, most likely related to the agonists and mice strains investigated. Indeed, the same TLR2 agonist had been reported by several studies to induce either Th2, Th1, or Th17 polarization.[57]

The most puzzling effect was observed with NOD1 liposomes, which were able to significantly reduce the tumor growth during the first month after TC-1 injection, but failed to increase the survival of tumor-bearing mice, even when injected at days 2-4. Given these observations, we suspected that NOD1 liposomes did not induce a long-term memory immune response, but rather a transient antitumor effect. This hypothesis was confirmed by the immune monitoring

20

of NOD1 liposomes-treated mice, which only had a limited number of IFN-γ-producing E7-specific T cells. Likewise, CD8-depleted mice treated with NOD1 liposomes presented the same number of tumor nodules than IgG-treated counterpart (Figure 3A). Then, we postulated that NOD1 liposomes may act *via* the activation of innate lymphoid subsets. Indeed, it has already been shown that NKT and NK cells express NOD1, and their stimulation with NOD1 agonist induces a strong IFN-γ production and enhances their cytotoxic activity.[58–60] However, the stimulation of innate subsets was not efficient enough in this model, which requires a strong and specific antitumor immunity to generate a solid therapeutic effect.

The differences in the efficiency of the three peptide-based liposomal vaccines might be further explained by their interaction with DCs. NOD1 **liposomes did not impact either the migration or the activation of DCs,** which corroborates the hypothesis that this construction acts independently of an adaptive cytotoxic immune response. Surprisingly, the least effective vaccine containing the TLR2/6 agonist induced the strongest maturation of skin DCs subsets (CD103⁻ and CD103⁺ DCs), known to be involved in the cross-presentation of tumor antigens.[24,61] However, no migration was measured with TLR2/6 liposomes, supporting the idea that this treatment enhances maturation of DCs that have already migrated to the lymph nodes. Indeed, liposomes are efficiently drained by the lymphatic system after s.c. administration.[20] In contrary, TLR4 liposomes did not promote CD86 expression beyond the levels usually observed in the skin-derived DCs found in lymph nodes of untreated mice. Nevertheless, we observed an outstanding migration of CD103⁻ DCs originating from the dermis. Therefore, peptide-based liposomal vaccines efficacy seems to correlate with an increase of DC migration from the skin, but not with an **additional a**ctivation of DCs within the draining lymph nodes.

5. Conclusion

The type of nanoparticular platform used in our study can overcome major drawbacks in the development of potent vaccines by facilitating: i) the selection of specific antigens, ii) the optimization of adjuvant composition and iii) the evaluation of antigen-adjuvant association, necessary to avoid unspecific immune responses or inefficient T helper polarization.[62] More importantly, we highlight the need to study adjuvant mechanism and identify immune features required to benefit from one type of vaccination composition. Thanks to this approach, we selected the TLR4 liposome **formulation in which each nanoparticle contains** the E7 tumor peptide, a universal T helper epitope and the TLR4 agonist MPLA. Such vaccine containing a universal helper peptide and a strong adjuvant could be the core of preformed personalized drugs, which will be associated at the bedside to neoantigenic peptides sequenced from patient biopsies.[63–64] Therefore, this tunable vaccination platform will facilitate vaccine manufacturing and may also be of interest for the conception of personalized medicines.

Conflicts of interest

The authors report no conflict of interest.

Appendix A. Supplementary materials

References

[1]   I. Mellman, G. Coukos, G. Dranoff, *Nature* **2011**, *480*, 480.

[2]   S. Farkona, E. P. Diamandis, I. M. Blasutig, *BMC Med.* **2016**, *14*, 73.

[3]   I. Melero, G. Gaudernack, W. Gerritsen, C. Huber, G. Parmiani, S. Scholl, N. Thatcher, J. Wagstaff, C. Zielinski, I. Faulkner, et al., *Nat. Rev. Clin. Oncol.* **2014**, *11*, 509.

[4]   K. K. Wong, W. A. Li, D. J. Mooney, G. Dranoff, *Adv. Immunol.* **2016**, *130*, 191.

[5]   H. Maeng, M. Terabe, J. A. Berzofsky, *Curr. Opin. Immunol.* **2018**, *51*, 111.

[6]   C. L. Slingluff, *Cancer J. Sudbury Mass* **2011**, *17*, 343.

[7]   M. Melssen, C. L. Slingluff, *Curr. Opin. Immunol.* **2017**, *47*, 85.

[8]   C. Maisonneuve, S. Bertholet, D. J. Philpott, E. De Gregorio, *Proc. Natl. Acad. Sci. U. S. A.* **2014**, *111*, 12294.

[9]   A. M. Didierlaurent, B. Laupèze, A. Di Pasquale, N. Hergli, C. Collignon, N. Garçon, *Expert Rev. Vaccines* **2017**, *16*, 55.

[10] D. O'Sullivan, T. Arrhenius, J. Sidney, M. F. Del Guercio, M. Albertson, M. Wall, C. Oseroff, S. Southwood, S. M. Colón, F. C. Gaeta, *J. Immunol. Baltim. Md 1950* **1991**, *147*, 2663.

[11] C. Schneider, M.H Van Regenmortel, *Arch. Virol.* 1992, *125*, 103–119.

[12] A. Roth, F. Rohrbach, R. Weth, B. Frisch, F. Schuber, W. S. Wels, *Br. J. Cancer* **2005**, *92*, 1421.

[13] J.-S. Thomann, B. Heurtault, S. Weidner, M. Brayé, J. Beyrath, S. Fournel, F. Schuber, B. Frisch, *Biomaterials* **2011**, *32*, 4574.

[14] P. R. Prabhu, D. Jayalekshmi, M. R. Pillai, *J Omcol.* **2012**, 2012:750270.

[15] X. Fan, K. Yu, J. Wu, J. Shao, L. Zhu, J. Zhang, *Tumour Biol. J. Int. Soc. Oncodevelopmental Biol. Med.* **2015**, *36*, 3043.

[16] A. Roth, S. Espuelas, C. Thumann, B. Frisch, F. Schuber, *Bioconjug. Chem.* **2004**, *15*, 541.

[17] B. Heurtault, P. Gentine, J.-S. Thomann, C. Baehr, B. Frisch, F. Pons, *Pharm. Res.* **2009**, *26*, 276.

[18] C. Jacoberger-Foissac, H. Saliba, C. Seguin, A. Brion, Z. Kakhi, B. Frisch, S. Fournel, B. Heurtault, *Int. J. Pharm.* 2019, *562*, 342.

[19] K. Y. Lin, F. G. Guarnieri, K. F. Staveley-O'Carroll, H. I. Levitsky, J. T. August, D. M. Pardoll, T. C. Wu, *Cancer Res.* **1996**, *56*, 21.

[20] C. Oussoren, G. Storm, *Adv. Drug Deliv. Rev.* **2001**, *50*, 143.

[21] C. Kelly, C. Jefferies, S.-A. Cryan, *J. Drug Deliv.* **2011**, *2011*, 727241.

[22] C. Mezière, M. Viguier M, H. Dumortier, R. Lo-Man, C. Leclerc, JG. Guillet, JP. Briand, S. Muller. *J. Immunol.* 1997, *159*, 3230.

[23] C. Burkhart, G. Freer, R. Castro, L. Adorini, KH. Wiesmüller, RM. Zinkernagel, H. Hengartner. *J. virol.* 1994, *68*, 1573.

[24] CD. Partidos, C. Kanse. *Mol Immunol.* 1997, *34*, 1105.

[25] A. K. Palucka, L. M. Coussens, *Cell* **2016**, *164,* 1233.

[26] B. T. Edelson, W. Kc, R. Juang, M. Kohyama, L. A. Benoit, P. A. Klekotka, C. Moon, J. C. Albring, W. Ise, D. G. Michael, et al., *J. Exp. Med.* **2010**, *207*, 823.

[27] B. Wylie, E. Seppanen, K. Xiao, R. Zemek, D. Zanker, S. Prato, B. Foley, P. H. Hart, R. A. Kroczek, W. Chen, et al., *Oncoimmunology* **2015**, *4*, e1019198.

[28] P. Stoitzner, C. H. Tripp, A. Eberhart, K. M. Price, J. Y. Jung, L. Bursch, F. Ronchese, N. Romani, *Proc. Natl. Acad. Sci.* **2006**, *103*, 7783.

[29] V. Flacher, C. H. Tripp, D. G. Mairhofer, R. M. Steinman, P. Stoitzner, J. Idoyaga, N. Romani, *EMBO Mol. Med.* **2014**, *6*, 1191.

[30] S. H. Apte, A. M. Redmond, P. L. Groves, S. Schussek, D. J. Pattinson, D. L. Doolan, *Eur. J. Immunol.* **2013**, *43*, 2707.

[31] G. Schreibelt, J. Tel, K. H. E. W. J. Sliepen, D. Benitez-Ribas, C. G. Figdor, G. J. Adema, I. J. M. de Vries, *Cancer Immunol. Immunother.* **2010**, *59*, 1573.

[32] C. Macri, E. S. Pang, T. Patton, M. O'Keeffe, *Semin. Cell Dev. Biol.* **2017**, *S1084-9521*, 30434.

[33] J. Liu, S. J. Blake, M. C. R. Yong, H. Harjunpää, S. F. Ngiow, K. Takeda, A. Young, J. S. O'Donnell, S. Allen, M. J. Smyth, et al., *Cancer Discov.* **2016**, *6*, 1382.

[34] S. A. Fisher, A. Cleaver, D. D. Lakhiani, A. Khong, T. Connor, B. Wylie, W. J. Lesterhuis, B. W. Robinson, R. A. Lake, *J. Transl. Med.* **2014**, *12*, 245.

[35] N. Grinshtein, B. Bridle, Y. Wan, J. L. Bramson, *Cancer Res.* **2009**, *69*, 3979.

[36] JM. Blander, R. Medzhitov. *Nature* 2006, *440*, 808.

[37] P. Yu, Y. Lee, W. Liu, T. Krausz, A. Chong, H. Schreiber, Y.-X. Fu, *J. Exp. Med.* **2005**, *201*, 779.

[38] W. Jing, J. A. Gershan, B. D. Johnson, *Blood* **2009**, *113*, 4449.

[39] J. B. A. G. Haanen, *Cell* **2017**, *170*, 1055.

[40] P. C. L. Trimble, M. P. Morrow, K. A. Kraynyak, X. Shen, M. Dallas, J. Yan, L. Edwards, R. L. Parker, L. Denny, M. Giffear, et al., *Lancet Lond. Engl.* **2015**, *386*, 2078.

[41] M. I. E. van Poelgeest, M. J. P. Welters, R. Vermeij, L. F. M. Stynenbosch, N. M. Loof, D. M. A. B. der Meer, M. J. G. Löwik, I. L. E. Hamming, E. M. G. van Esch, B. W. J. Hellebrekers, et al., *Clin. Cancer Res.* **2016**, *22*, 2342.

[42] D.-W. Liu, Y.-P. Tsao, J. T. Kung, Y.-A. Ding, H.-K. Sytwu, X. Xiao, S.-L. Chen, *J. Virol.* **2000**, *74*, 2888.

[43] W.-F. Cheng, C.-F. Hung, C.-Y. Chai, K.-F. Hsu, L. He, M. Ling, T.-C. Wu, *J. Virol.* **2001**, *75*, 2368.

[44] A. Lamikanra, Z. K. Pan, S. N. Isaacs, T. C. Wu, Y. Paterson, *J. Virol.* **2001**, *75*, 9654.

[45] J. Li, Y. Sun, A. Garen, *Proc. Natl. Acad. Sci.* **2002**, *99*, 16232.

[46] C. Jindra, B. Huber, S. Shafti-Keramat, M. Wolschek, B. Ferko, T. Muster, S. Brandt, R. Kirnbauer, *PLoS ONE* **2015**, *10*, e0138722.

[47] M. Sadraeian, M. J. Khoshnood Mansoorkhani, M. Mohkam, S. Rasoul-Amini, M. Hesaraki, Y. Ghasemi, *Cell J. Yakhteh* **2013**, *15*, 176.

[48] R. Mikyšková, I. Štěpánek, M. Indrová, J. Bieblová, J. Šímová, I. Truxová, I. Moserová, J. Fučíková, J. Bartůňková, R. Špíšek, et al., *Int. J. Oncol.* **2016**, *48*, 953.

[49] M. Nizard, H. Roussel, M. O. Diniz, S. Karaki, T. Tran, T. Voron, E. Dransart, F. Sandoval, M. Riquet, B. Rance, et al., *Nat. Commun.* **2017**, *8*, 15221.

[50] L. Bialkowski, A. van Weijnen, K. V. der Jeught, D. Renmans, L. Daszkiewicz, C. Heirman, G. Stangé, K. Breckpot, J. L. Aerts, K. Thielemans, *Sci. Rep.* **2016**, *6*, 22509.

[51] A. Yang, S. Peng, E. Farmer, Q. Zeng, M. A. Cheng, X. Pang, T.-C. Wu, C.-F. Hung, *Cell Biosci.* **2017**, *7*, 46.

[52] C.-C. Wu, F.-C. Wu, Y.-T. Hsu, Y.-C. Hsiao, Y.-C. Yang, C. A. Chang, C.-L. Chang, *Oncotarget* **2017**, *8*, 33024.

[53] I.-J. Chen, C.-F. Yen, K.-J. Lin, C.-L. Lee, Y.-K. Soong, C.-H. Lai, C.-T. Lin, *Reprod. Sci. Thousand Oaks Calif* **2011**, *18*, 687.

[54] Y.-L. Li, X.-H. Qiu, C. Shen, J.-N. Liu, J. Zhang, *Oncol. Rep.* **2010**, *24*, 1323.

[55] Y.-L. Li, Z.-L. Ma, Y. Zhao, J. Zhang, *Oncol. Lett.* **2015**, *9*, 1851.

25

[56] S. Zwaveling, S. C. Ferreira Mota, J. Nouta, M. Johnson, G. B. Lipford, R. Offringa, S. H. van der Burg, C. J. M. Melief, *J. Immunol. Baltim. Md 1950* **2002**, *169*, 350.

[57] A. P. Basto, A. Leitão, *J. Immunol. Res.* **2014**, *2014*, 619410.

[58] T. Selvanantham, N. K. Escalante, M. Cruz Tleugabulova, S. Fiévé, S. E. Girardin, D. J. Philpott, T. Mallevaey, *J. Immunol. Baltim. Md 1950* **2013**, *191*, 5646.

[59] F. Qiu, A. Maniar, M. Quevedo Diaz, A. I. Chapoval, A. E. Medvedev, *Innate Immun.* **2011**, *17*, 375.

[60] G. E. Pluhar, C. A. Pennell, M. R. Olin, *Crit. Rev. Immunol.* **2015**, *35*, 153.

[61]   M.-L. del Rio, J.-I. Rodriguez-Barbosa, E. Kremmer, R. Förster, *J. Immunol. Baltim. Md 1950* **2007**, *178*, 6861.

[62] C. Gouttefangeas, H.-G. Rammensee, *Cancer Immunol. Immunother.* **2018**, 1.

[63] U. Sahin, Ö. Türeci, *Science* **2018**, *359*, 1355.

[64] H. K. Charlton Hume, L. H. L. Lua, *Vaccine* **2017**, *35*, 4480.

Table 1. Composition of formulated liposomes

Liposomal construct	Lipid bilayer		Peptides	
	Composition	**Molar ratio**	**Compo-sition**	**Molar ratio**
Plain lp.	PC/PG/Chol	54/13/33	HA/E7	
TLR2/6 lp. (HA-E7-Pam$_2$CAG)	PC/PG/Chol/DPGmal/Pam$_2$CAG	50.9/13/33/3/0.1	HA/E7	
TLR4 lp. (HA-E7-MPLA)	PC/PG/Chol/DPGmal/MPLA	51/13/33/3/0.007	HA/E7	0.75/0.75
NOD1 lp. (HA-E7-C12iEDAP)	PC/PG/Chol/DPGmal/C12iEDAP	50.8/13/33/3/0.3	HA/E7	

PC: phosphatidylcholine, PG: phosphatidylglycerol, Chol: cholesterol, DPGmal: dipalmitoyl glycerol-maleimide, Pam$_2$CAG: dipalmitoyl-cysteine-alanyl-glycine, MPLA: monophosphoryl lipid A, C12iEDAP: acylated derivative of the dipeptide γ-D-Glu-mDAP.

Table 2. Physicochemical properties of liposome-based constructs. Results are the mean of at least 8 independent formulations (with 3 consecutive measurements in each preparation). Measurements were performed after thawing at room temperature.

Vaccine constructs	Size (Intensity)		Zeta potential (mV)	Peptide coupling rate (%)	Adjuvant (dose/ injection)*	HA and E7 peptides (dose/ injection)
	Average diameter (nm)	PDI				
Plain lp.	70±13	0.187	-60±8	-	-	-
TLR2/6 lp.	76±14	0.236	-51±6	78	2.4 µg	
TLR4 lp.	89±20	0.215	-63±6	80	0.2 µg	15 µg
NOD1 lp.	83±16	0.216	-61±6	83	2.2 µg	

PDI: polydispersity index *The optimal dosage of each adjuvant was already determined in a previous study.[23]

Fig. 1. Therapeutic efficacy of adjuvanted liposomal vaccines in an orthotopic lung tumor model. (A-C) Antitumor activity at various stage of cancer progression, delay of the injection schedule. After an i.v. injection of 1.10^5 TC-1 cells, mice received two s.c. immunizations (2 injections, 2-d interval) of plain liposomes at days 2 and 4, or liposomal constructs containing TLR2/6 (A), TLR4 (B), or NOD1 (C) agonists at different times, beginning at day 2 until day 14 after tumor implantation. At day 28, mice lungs were collected, contrasted by intratracheal injection of 15% india ink and decolorated in a Fekete solution overnight. Data represent mean±SEM of tumor nodules count, n>7. (D-E) Survival rate of mice after therapeutic vaccination. After tumor cells injection, s.c. administrations of liposomal constructs were performed at days 2 and 4 (D) or days 10 and 12 (E), **as represented by the black arrows on the figures.** Percentages of mice survival are shown. Statistically differences between groups were determined using a one-way ANOVA or a log rank test.
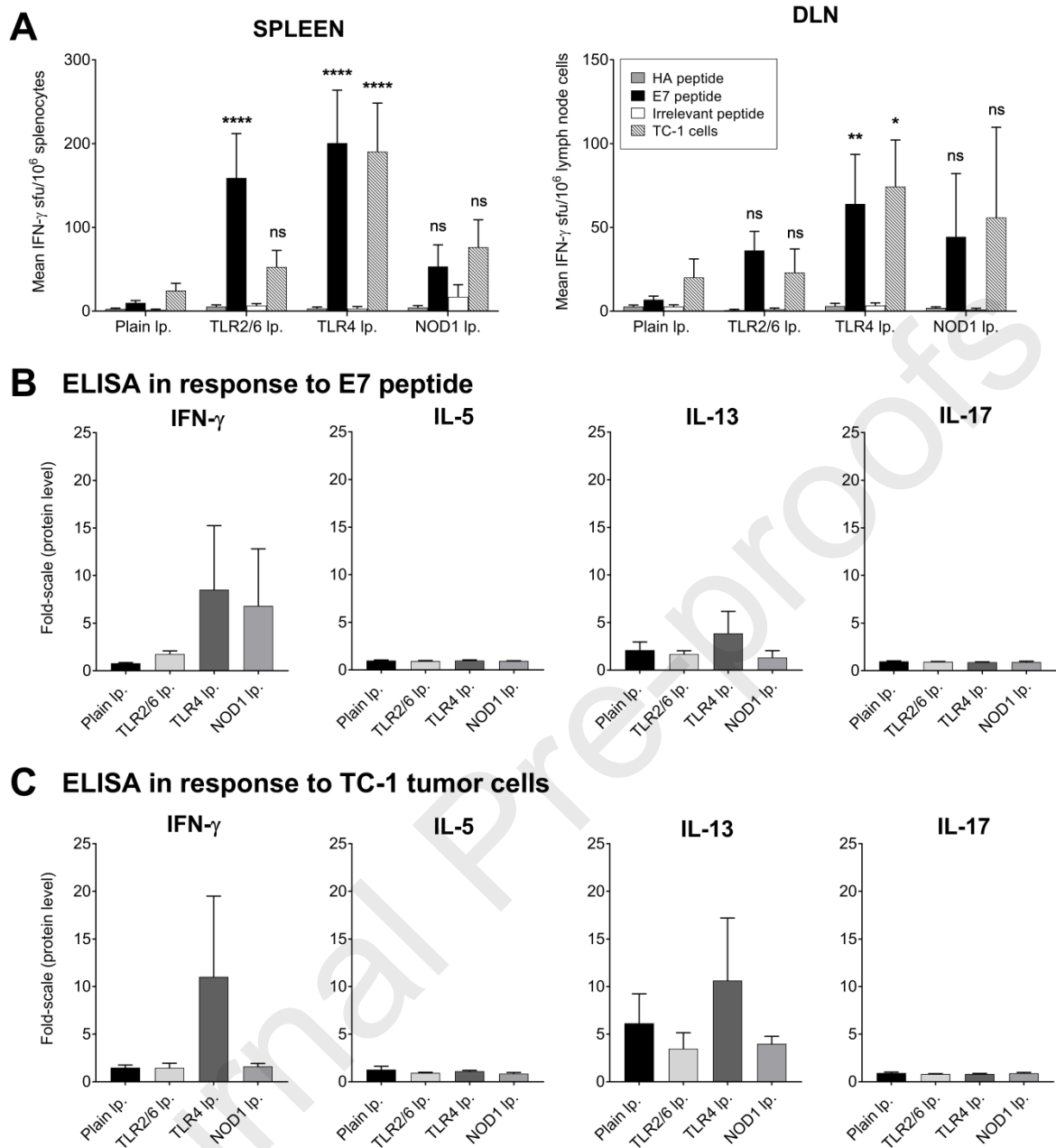
Fig. 2. Monitoring of the antitumor immunity. (A) Evaluation of adaptive cellular immune response after therapeutic vaccination. Following the classic schedule (vaccination at days 2/4), mice were treated with plain liposomes (negative control, n=11) or liposomal constructs containing TLR2/6 (n=8), TLR4 (n=5), or NOD1 (n=4) agonists as adjuvants. At day 28, spleen and DLNs were collected and pooled according to treatment groups. The number of IFN-γ producing cells was measured by ELISpot after 24 h in presence of HA, E7, irrelevant peptides

(10 µg/mL) or 125.10^3 TC-1 tumor cells. Results are expressed as mean±SEM of IFN-γ spots/10^6 cells. (B-C) Cytokines production by splenocytes in response to E7 peptide or TC-1 tumor cells. ELISA for IFN-γ, IL-5, IL-17 and IL-13 cytokines were performed after 72 h culture period of splenocytes supernatants from mice treated with different vaccine candidates **28 days before,** in presence of E7 peptide (B) or TC-1 tumor cells (C) (n=3). Cells incubated in medium alone were used to calculate the relative fold change in cytokine production. "n" represents the number of organ batch from independent experiments. Significant differences were determined by an ANOVA statistical test.
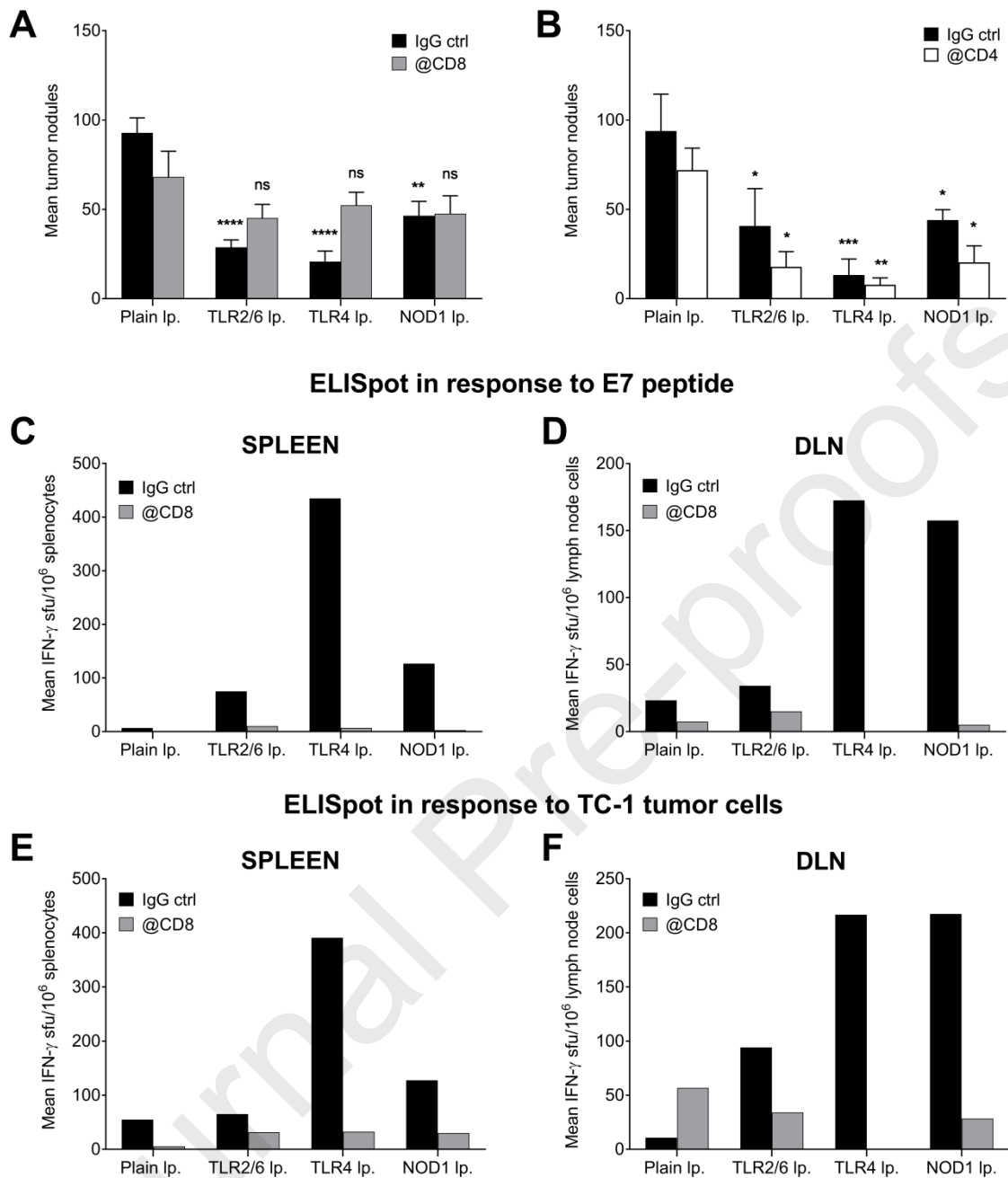
ELISpot in response to E7 peptide

ELISpot in response to TC-1 tumor cells

Fig. 3. CD8+ and CD4+ depletion impact on peptide-based vaccines efficacy. Prior to tumor injection and vaccination (classic schedule), mice received i.p. injection of 200 μg rat IgG (negative control), anti-CD4 or anti-CD8α depleting antibodies, followed by a weekly challenge to maintained depletion. (A-B) Antitumor efficacy after T cell depletion. At day 28, mice lungs

from CD8α (A) or CD4 (B) depleting experiments were collected, contrasted by intracheal injection of 15% india ink and decolorated in a Fekete solution overnight. Data represent mean±SEM of tumor nodules count, n=8 or n=4, respectively. Statistically differences between groups were determined using a two-way ANOVA. (C-F) Inhibition of specific immune response after CD8^{+} depletion (ELISpot in response to E7 peptide and TC-1 tumor cells). At day 28, spleen (C, E) and DLNs (D, F) from mice treated with rat IgG or CD8α antibodies were collected and pooled according to treatment groups. The number of IFN-γ producing cells was measured by ELISpot after 24 h in presence of E7 peptide (C-D) and TC-1 tumor cells (E-F). Results are expressed as mean±SEM of IFN-γ spots/10^6 cells (n>3, **C-F data representative of 3 independent experiments)**.
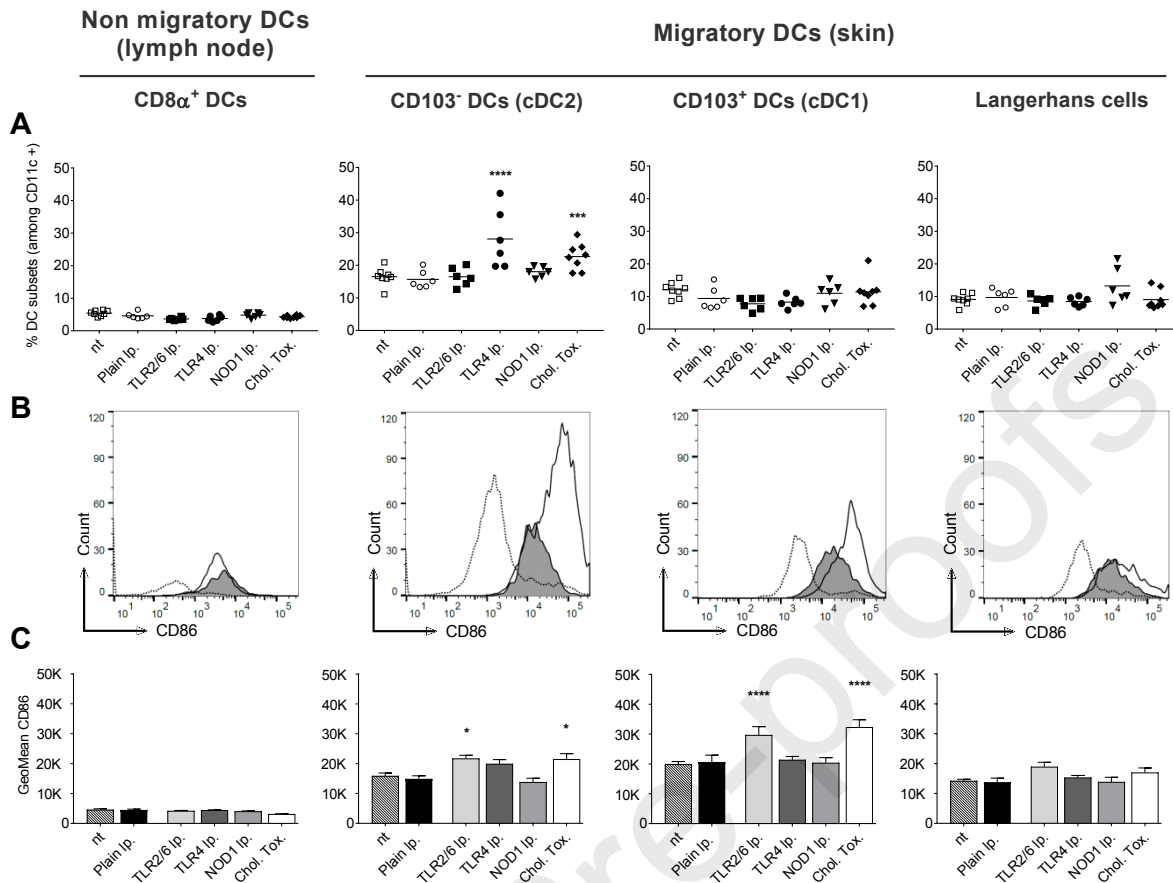
Fig. 4. Migration and activation of skin DCs after peptide-based vaccines s.c. injection. Tumor-free C57BL/6J mice were left untreated (nt) or received a s.c. injection of plain liposomes, TLR2/6 liposomes, TLR4 liposomes, NOD1 liposomes or cholera toxin (Chol. Tox.) into their right flank. Flow cytometric analysis of DLN resident or migratory DC subsets were performed 48 h after immunization. Gating strategy for CD8α⁺, CD103⁻, CD103⁺ and Langerhans DCs are shown in Figure S3. (A) Frequency of DC subsets among CD11c⁺ cells. Each data point represents measurement obtained in 6-8 mice from two independent experiments. (B) Representative comparison of CD86 expression from an untreated mouse (shaded histograms), a mouse treated with Chol. Tox. (empty histograms with solid lines) and FMO control (histograms with dotted lines) (C) Mean fluorescence intensity of CD86 surface density on four different DC subsets, from 5 treatment groups. Data are the mean±SEM of two independent

34

experiments, with at least 3 mice per condition. Significant differences were determined by a

2-way ANOVA statistical test.

Induction of a Strong and Persistent Antitumor Immune Response using Monophosphoryl Lipid A Adjuvanted Liposomal Vaccines
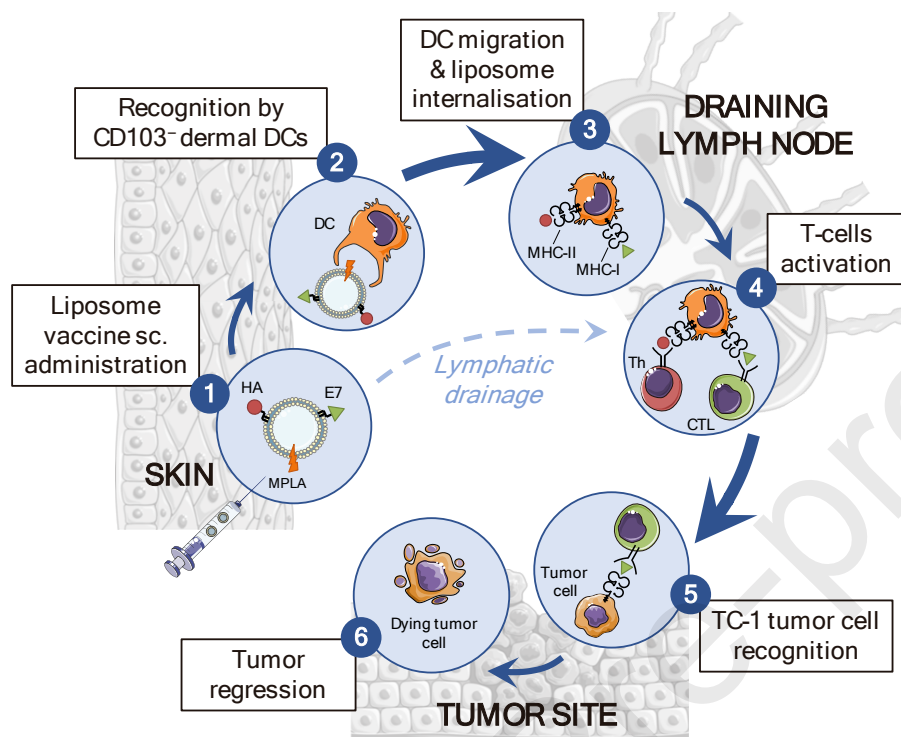
Graphical abstract. TLR4 liposome containing MPLA (adjuvant), Th (HA) and tumor specific (E7) peptides is a very potent cancer vaccine capable of inducing a strong cytotoxic immune response against tumor cells. The subcutaneous administration of the vaccine (1) induce the migration of CD103⁻ dermal DC into the draining lymph nodes (2-3) followed by the differentiation of Th and CTL lymphocytes (4) leading to the specific recognition and destruction of tumor cells (5-6).